

---



---

**ELEMENTARY PARTICLES AND FIELDS**  
**Experiment**

---



---

## Capabilities of the Gamma-400 Gamma-ray Telescope for Observation of Electrons and Positrons in the TeV Energy Range

A. A. Leonov<sup>1),2)\*</sup>, A. M. Galper<sup>1),2)</sup>, N. P. Topchiev<sup>2)</sup>, A. V. Bakaldin<sup>2),3)</sup>,  
M. D. Kheimits<sup>1)</sup>, A. V. Mikhailova<sup>1)</sup>, V. V. Mikhailov<sup>1)</sup>, and S. I. Suchkov<sup>2)</sup>

Received July 15, 2019; revised July 15, 2019; accepted July 15, 2019

**Abstract**—The space-based GAMMA-400 gamma-ray telescope will measure the fluxes of gamma rays in the energy range from  $\sim 20$  MeV to several TeV and cosmic-ray electrons and positrons in the energy range from several GeV to several TeV to investigate the origin of gamma-ray sources, sources and propagation of the Galactic cosmic rays and signatures of dark matter. The instrument consists of an anticoincidence system, a converter-tracker (thickness one radiation length,  $1 X_0$ ), a time-of-flight system, an imaging calorimeter ( $2 X_0$ ) with tracker, a top shower scintillator detector, an electromagnetic calorimeter from CsI(Tl) crystals ( $16 X_0$ ) with four lateral scintillation detectors and a bottom shower scintillator detector. In this paper, the capability of the GAMMA-400 gamma-ray telescope for electron and positron measurements is analyzed. The bulk of cosmic rays are protons, whereas the contribution of the leptonic component to the total flux is  $\sim 10^{-3}$  at high energy. The special methods for Monte Carlo simulations are proposed to distinguish electrons and positrons from proton background in the GAMMA-400 gamma-ray telescope. The contribution to the proton rejection from each detector system of the instrument is studied separately. The use of the combined information from all detectors allows us to reach a proton rejection of up to  $\sim 1 \times 10^4$ .

**DOI:** 10.1134/S1063778819660359

### 1. INTRODUCTION

The GAMMA-400 instrument [1–3] was developed to address a broad range of scientific goals, such as search for signatures of dark matter, studies of galactic and extragalactic gamma-ray sources, galactic and extragalactic diffuse emission, gamma-ray bursts. Meanwhile, the instrument allows us to measure also high-energy charged particles such as protons, electrons and positrons. High-precision measurement of total electron and positron flux is an important task in the light of recent data from the DAMPE [4], CALET [5], AMS-02 [6] and Fermi-LAT [7] experiments, which found several features in the spectral shape of their flux and are weakly consistent with each other. GAMMA-400 is equipped with a rather thick calorimeter and has a larger geometric acceptance, which will provide high statistics up to several TeV. It is important also, that the instrument will operate in space without the occultation of the

Earth. This paper describes the performance of the GAMMA-400 instrument for measurements of the total electron flux (electrons and positrons together) from main aperture with field-of-view of  $\pm 45^\circ$ . Detecting electron and positron fluxes from lateral direction using electromagnetic calorimeter ( $54 X_0$ ) with four lateral detectors will be described in another paper.

### 2. INSTRUMENT

The physical scheme of the GAMMA-400 gamma-ray telescope is shown in Fig. 1. GAMMA-400 consists of plastic scintillation top and lateral detectors (AC), which make up an anticoincidence system; a converter-tracker ( $C$ ); plastic scintillation detectors ( $S1$  and  $S2$ ,  $1 \times 1$  m and  $1 \times 0.8$  m) forming the Time-of-Flight system (ToF); an imaging calorimeter with tracker (CC1); a plastic scintillation detector ( $S3$ ) forming an additional trigger for high-energy gamma and charged particle detection; an electromagnetic calorimeter (CC2) with four lateral scintillation detectors (SL CC2); a plastic scintillation detector ( $S4$ ). The anticoincidence detectors surrounding the converter-tracker serve to distinguish gamma-ray events from the much more numerous charged-particle events. Converter-tracker and imaging

<sup>1)</sup>National Research Nuclear University MEPhI (Moscow Engineering Physics Institute), Russia.

<sup>2)</sup>P.N. Lebedev Physical Institute of the Russian Academy of Sciences, Moscow, Russia.

<sup>3)</sup>Scientific Research Institute for System Analysis of the Russian Academy of Sciences, Moscow, Russia.

\*E-mail: aaleonov@mephi.ru

calorimeter tracker information is applied to precisely determine the direction of each incident gamma and the calorimeter measurements are used to determine its energy. The ToF system, where detectors  $S1$  and  $S2$  are separated by 500 mm, allows distinguishing the upward or downward arriving particle direction. The scintillation detector  $S4$  improves the separation of electromagnetic and hadronic showers. All scintillation detectors ( $S1$ ,  $S2$ ,  $S3$ ,  $S4$  and  $AC$ ) consist of 2 independent layers, each one with a thickness of 1 cm.

The imaging calorimeter  $CC1$  consists of a CsI(Tl) crystal layer and of double  $(x, y)$  fiber coordinate detectors; the electromagnetic calorimeter  $CC2$  consists of CsI(Tl) crystals with the dimensions of  $36 \times 36 \times 300$  mm. The long axis of these crystals is “vertical” (parallel to the axis of the instrument). The total converter-tracker thickness is about 1 radiation length  $X_0$ . The thicknesses of  $CC1$  and  $CC2$  are  $2 X_0$  and  $16 X_0$ , respectively. The total calorimeter thickness is  $\sim 18 X_0$  or  $\sim 1$  nuclear interaction lengths  $\lambda_0$ . Using a thick calorimeter allows us to extend the energy range up to several TeV and reach an energy resolution better than 1% for electrons above 100 GeV. The design of the instrument was optimized to achieve optimal characteristics for angular and energy resolution of gamma rays in energy interval from 20 MeV to 100 GeV. The main trigger of the instrument is  $\overline{AC} \times \text{ToF}$ . At high energy, the backscattering of secondary particles, produced in calorimeter  $CC2$ , can hit the  $AC$  detectors. To keep high efficiency of gamma rays with energy above 10 GeV and reject backscattering, an additional trigger signal will be used:

$$\text{ToF} \times S3(E_{\text{THRESHOLD}}), \quad (1)$$

where  $E_{\text{THRESHOLD}}$  is the energy threshold. Using this trigger the registration of charged particles is also available. The geometric factor of the instrument is about  $1 \text{ sr m}^2$ , dead time is about 1 ms.

It is necessary to note that different physical schemes in [1–3] are explained by different masses of scientific payload for different launch vehicles for the GAMMA-400 space observatory. The instrument will be launched into a highly elliptical orbit (with an apogee of 300000 km and a perigee of 500 km, with an inclination of  $51.4^\circ$ ), with 7 days orbital period. The volume of transmitted information will reach 100 GB per day. The expected lifetime of the observatory is  $\sim 7$  years.

### 3. ELECTRON AND POSITRON IDENTIFICATION

Simulations of the electron efficiency and the rejection factor of protons from electrons in GAMMA-400 were calculated on the base of GEANT4.10

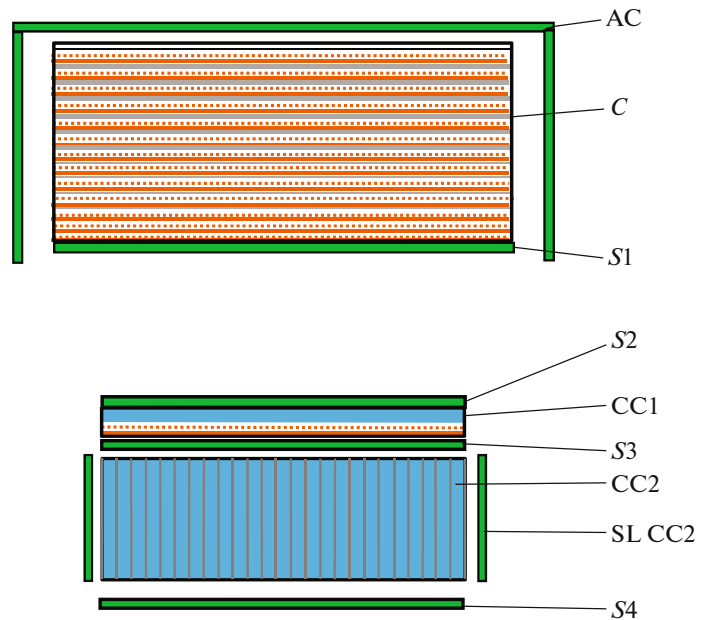


**Fig. 1.** The physical scheme of gamma-ray telescope GAMMA-400.

toolkit (<http://geant4.cern.ch>). All these calculations were performed in the energy range from 1 GeV to 1 TeV both for electrons and protons.

Only those events with energy deposition  $E$ , which satisfy the additional trigger condition  $\text{ToF} \times S3(E > E_{\text{THRESHOLD}})$ , were considered in the analysis. Figure 2 shows the efficiency for electrons (a) and protons (b) for different thresholds of the detector  $S3$ . Taking into account the known spectrum of protons [8], a value of  $E_{\text{THRESHOLD}}$  between 30–100 MeV will provide a count rate of background protons of less than 50% of the total rate. The threshold value 100 MeV was approved in view of trade-in between proton rejection from gamma channel and recording efficiency of high-energy gamma associated with backplash.

To reject protons from electrons further, the information from  $S1$ ,  $S4$ ,  $CC1$ , and  $CC2$  was used. Every detector is considered as a separate layer, and the ability of each layer to reject the proton contamination in different energy ranges was studied individually. In principle, an interacting proton with energy more than 100 GeV could imitate a 100-GeV electron, since it can release the same energy deposit in the GAMMA-400 calorimeter. The rejection factor at 100 GeV is then calculated as the ratio of the number of initial protons with energy more than 100 GeV (assuming that the proton energy spectrum power-index is  $-2.7$ ) to the number of events identified as electrons with energy  $100 \pm 2$  GeV (taking into account that the GAMMA-400 energy resolution is of

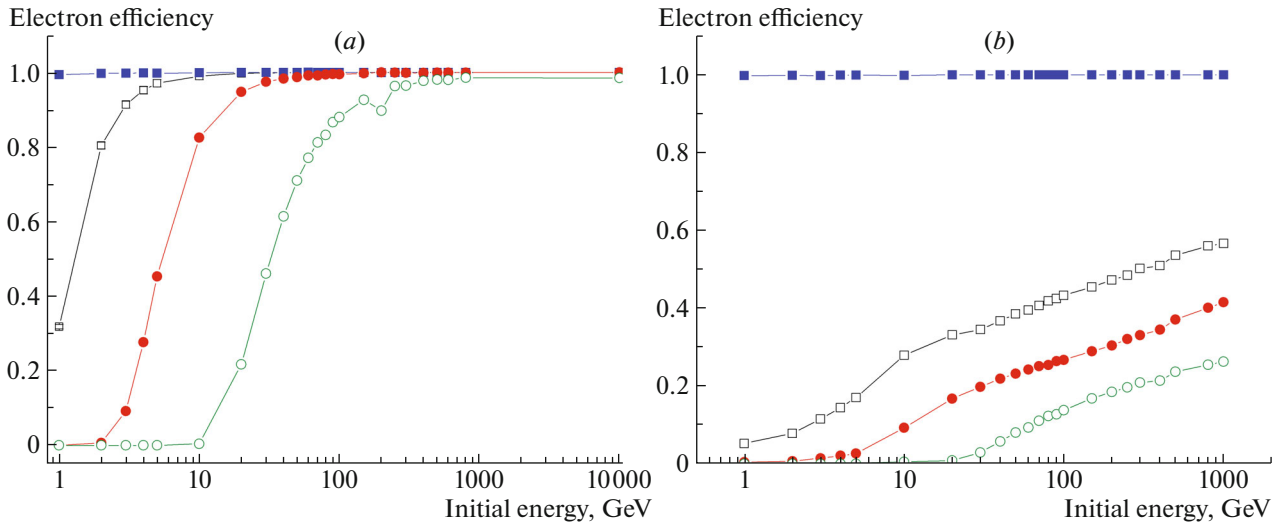


**Fig. 2.** Efficiency of electron (a) and proton (b) detection as function of the energy of particles for different energy thresholds in the S3 detector (filled square 0, open square 32 MeV, filled circle 100 MeV, open circle 300 MeV).

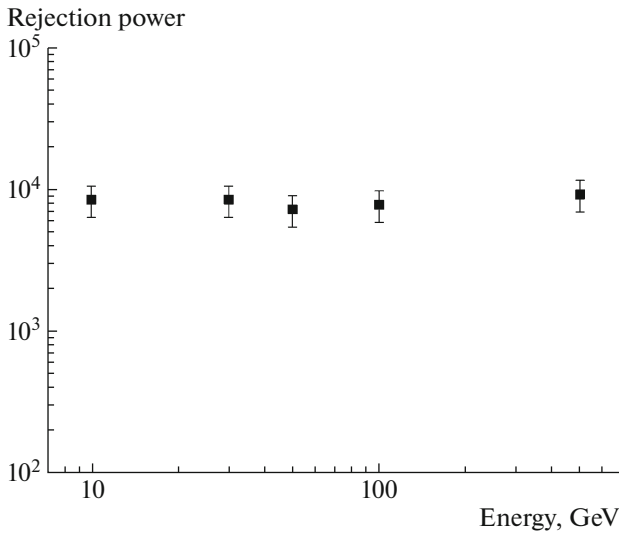


**Fig. 3.** Rejection factor of protons for the electron channel as function of energy.

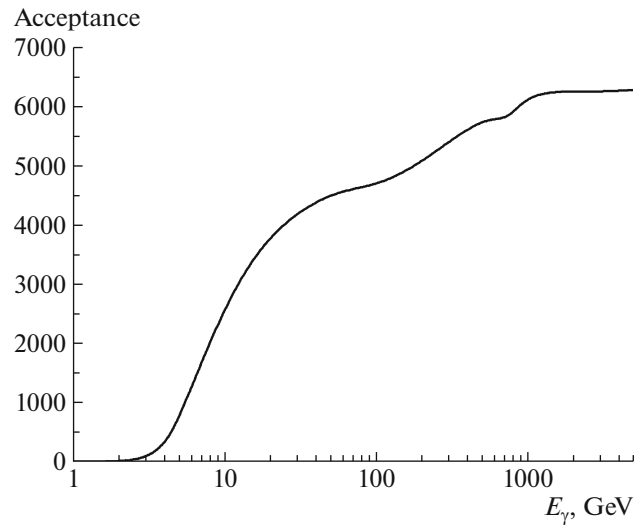


**Fig. 4.** The energy dependence of GAMMA-400 acceptance [ $\text{cm}^2 \text{sr}$ ] with the additional trigger signal (1) for electrons + positrons measurements.

about 2%). This approach is specific for the instrument configuration, considering the total depth of the materials ( $\sim 1.0 \lambda_0$ ), which determines the probability of proton nuclear interactions inside the calorimeter, the mean energy of protons that might imitate 100-GeV electrons, and the energy resolution.

Applying the threshold value 100 MeV for additional trigger (1) provides the rejection factor of protons  $\sim 3.3$ .

#### 4. RESULTS

To take into account the fact that the hadronic cascade begins to develop deeper inside the instrument than the electromagnetic one, the signals in S1

and S2 are considered. The difference in electron and proton distributions provides the rejection factor  $\sim 3$ .

Additional rejection is obtained when analyzing the CC2 signals. The first criterion is based on the difference of the transversal size for hadronic and electromagnetic showers. Analyzing the distributions of protons and electrons for RMS in CC2, it is possible to obtain a rejection factor  $\sim 15$ . The second criterion concerns the distribution of energy release in the hadronic and electromagnetic showers. Analyzing the distributions of protons and electrons for the ratio between a signal in the crystal containing the axis cascade and the value of the total signal in CC2

for incoming electrons and protons:  $E_{\text{MAX}}^{\text{CC2}}/E_{\text{TOT}}^{\text{CC2}}$ , it is possible to obtain a rejection factor  $\sim 1.6$ .

The information from *S4* located at the bottom of the calorimeter provides a strong intrinsic rejection factor for protons, due to the difference in attenuation for hadronic and electromagnetic cascades. Electromagnetic showers initiated by an electron with initial energy up to  $\sim 100$  GeV are fully contained inside a calorimeter with the thickness  $16 X_0$ , while protons leave the calorimeter taking away a considerable part of the energy and produce a signal in *S4*. By selecting events with signals in *S4* less than 40 MeV, it is possible to suppress protons with a factor of  $\sim 3.1$ . It turns out that a significantly more powerful criterion can be defined with distributions of the ratio of the signal in *S4* to the total signal in CC2. Applying this criterion, the rejection factor  $\sim 17$  is achieved.

The differences in the proton and electron cascade transverse size are also used when analyzing information from silicon strips in CC1. The application of this criterion provides a rejection factor of  $\sim 2$ .

Using all presented criteria jointly, the total rejection of protons for 100-GeV electrons is  $\sim 10^4$ .

A similar analysis was applied for the electron channels of different energies. The energy dependence of the rejection factor for protons in the electron channel is presented in Fig. 3. This value is  $\sim 10^4$  for the whole energy range of interest, providing the possibility to measure electron + positron fluxes. The energy dependence of the GAMMA-400 acceptance [ $\text{cm}^2 \text{ sr}$ ] with the additional trigger signal (1) for electrons + positrons measurements is presented in Fig. 4. For such acceptance the expected value of the count rate of electrons + positrons will be  $\sim 1$  Hz.

## 5. CONCLUSION

The GAMMA-400 gamma-ray telescope will measure the energy spectrum of electrons + positrons in the range from  $\sim 1$  GeV to  $\sim 10$  TeV. The capability of the GAMMA-400 gamma-ray telescope for measurements of electrons and positrons was analyzed

using Monte-Carlo simulations. The contribution to the proton rejection from each detector system of the GAMMA-400 instrument is studied separately. The use of the combined information from all detectors allows us to reach a proton rejection up to  $\sim 1 \times 10^4$ .

## FUNDING

This work was partially supported by State Corporation ROSCOSMOS (contract no. 024-5004/16/224) and by the RFBR project no. 18-02-00656.

## REFERENCES

1. A. Galper, O. Adriani, R. L. Aptekar, I. V. Arkhangel'skaja, A. I. Arkhangel'skiy, M. Boezio, V. Bonvicini, K. A. Boyarchuk, Yu. V. Gusakov, M. O. Farber, M. I. Fradkin, V. A. Kachanov, V. A. Kaplin, M. D. Kheymits, A. A. Leonov, F. Longo, et al., *Adv. Space Res.* **51**, 297 (2013).
2. N. P. Topchiev, A. M. Galper, V. Bonvicini, O. Adriani, R. L. Aptekar, I. V. Arkhangel'skaja, A. I. Arkhangel'skiy, A. V. Bakaldin, L. Bergstrom, E. Berti, G. Bigongiari, S. G. Bobkov, M. Boezio, et al., *J. Phys.: Conf. Ser.* **675**, 032009 (2016).
3. N. Topchiev, A. M. Galper, I. V. Arkhangel'skaja, A. I. Arkhangel'skiy, A. V. Bakaldin, I. V. Chernysheva, O. D. Dalkarov, A. E. Egorov, Yu. V. Gusakov, M. D. Kheymits, A. A. Leonov, P. Yu. Naumov, N. Yu. Pappé, M. F. Runsto, Yu. I. Stozhkov, S. I. Suchkov, et al., *EPJ Web Conf.* **208**, 14004 (2019).
4. DAMPE Collab. (G. Ambrosi et al.), *Nature* **552**, 63 (2017).
5. O. Adriani et al. (CALET Collab.), *Phys. Rev. Lett.* **120**, 261102 (2018).
6. M. Aguilar et al. (AMS Collab.), *Phys. Rev. Lett.* **122**, 101101 (2019).
7. S. Abdollahi et al. (The Fermi-LAT Collab.), *Phys. Rev. D* **95**, 082007 (2017).
8. O. Adriani, G. C. Barbarino, G. A. Bazilevskaya, R. Bellotti, M. Boezio, E. A. Bogomolov, M. Bongi, V. Bonvicini, S. Bottai, A. Bruno, F. Cafagna, D. Campana, R. Carbone, P. Carlson, M. Casolino, G. Castellini, et al., *Phys. Rep.* **544**, 323 (2014).